OZONE FUNCTIONALISED CARBON NANOTUBES FOR STRUCTURAL SUPERCAPACITORS

Benjamin J. Mapleback[1], Patrick C. Howlett[2] and Andrew N. Rider[3]

[1] Platforms, Defence Science and Technology Group, Melbourne, Australia,
benjamin.mapleback1@defence.gov.au
[2] Institute of Frontier Materials, Deakin University, Burwood, Australia,
patrick.howlett@deakin.edu.au
[3] Platforms, Defence Science and Technology Group, Melbourne, Australia,
andrew.rider@defence.gov.au

Keywords: Supercapacitor, carbon nanotubes and ozone

Abstract

Successful incorporation of supercapacitors into load bearing composite structures enables significant improvements to the size, weight and power (SWaP) of aerial vehicles. Developing materials and novel structural supercapacitor designs suited for use in high performance composites is required to ensure mechanical performance is maintained while adding useful energy storage. Localised structural supercapacitors use electrodes and separators across the entire laminate, however, the electrolyte is dispensed only in specific areas. This design requires improvements made to materials both inside and outside the electrochemically active region. Ozone functionalised carbon nanotube (CNT) mat electrodes and pre-impregnated low weight woven glass fibre is used as the separator with EMIm TFSI ionic liquid electrolyte. Functionalised CNT mats were mechanically shear tested to ascertain their mechanical impact to the regions outside of the active region, leading to a finding that 6 hours of ozone functionalisation increased shear strength to 118 MPa from 98 MPa in the composite without CNT mats. Then supercapacitors were incorporated into highly optimised aerospace composites to undergo mechanical shear testing and fractography to determine failure modes inside, outside and adjacent to the active region of the supercapacitor. Outside of the active region the composite retained an average shear strength of 84 MPa (54 MPa was retained within the active region). Residual epoxy within the glass fibre ply formed structural connections in the glass fibre cloth and with the adjacent CNT mat electrodes greatly improving strength. Electrochemical results of a new localised composite structural supercapacitor (SSC) using 6 h ozone functionalised CNT mat electrodes and a boron nitride separator are presented with impressive energy of 12.8 Wh kg^{-1} at 98.5 W kg^{-1} and power of 3790 W kg^{-1} at 0.6 Wh kg^{-1} with an electrode mass totalling 18.5 mg. Localising the SSC improves energy storage within the active region while maintaining mechanical performance outside of the active area. This enables more options for the design of aerospace components with added energy storage.

1 INTRODUCTION

It is generally appreciated that future vehicles with advanced technology will have more demanding energy requirements. Battery technology continues to be developed but they still leave capability gaps with regard to high-power electrical energy supply. The high power density supercapacitor is used to support the high energy density batteries, which are not able to safely charge or discharge at rates high enough for some systems. Additionally, space and weight can be saved by utilising existing space for the integration of additional high-power energy storage in a hybrid electric power configuration.

One approach is to incorporate supercapacitors into existing load bearing fibre-reinforced polymer (FRP) composite structures in a way that is not significantly detrimental to their mechanical performance. This has been explored through the use of graphene, carbon aerogel and carbon nanotubes attached to carbon fibres as electrodes [1]–[4], adding metal oxides to carbon fibres as electrodes [5]–[8], and using interwoven carbon nanotube (CNT) mats [9]–[12] as electrode materials for composite structural supercapacitors (SSCs). These approaches are able to provide good mechanical performance but still require further developments to improve their electrochemical performance. Oxygen

functionalisation of these CNTs with redox active groups is possible by ozonolysis [13], [14], which increases both electrochemical [14] and mechanical [15] performance. Limited work has been done to explore how aqueous based ozone functionalisation of CNTs affects electrochemical performance of ionic liquid (IL) supercapacitors and mechanical performance of supercapacitors within aerospace composites.

In this work supercapacitors are manufactured using components with good individual mechanical properties. This ensures that high-power energy storage can be added to load bearing FRP composite structures without significantly degrading their mechanical performance. The integrated SSC electrodes are a self-standing mat composed of interconnected CNT mat with metallic iron and iron carbide nanoparticles, which have previously been investigated by this group [10]. Localising the SSC within the composite has shown promising electrochemical results with ionogels and IL electrolytes [12]. These CNT mats are ozone treated in water to add redox active functional groups to the CNTs, as well as, oxidizing the iron species present in the CNT mat. Thin woven pre-impregnated (prepreg) glass fibre is used as electrical separating layers which are laid up into the laminate. Room temperature IL will be used as the electrolyte material as these materials can withstand epoxy curing temperatures and have very low vapour pressures, ensuring they will not vaporize under vacuum. These supercapacitor devices are to be cured into aerospace carbon fibre prepreg composites using standard vacuum bagging and autoclave curing techniques. The novelty of the proposed concept is in the use of self-standing CNT mats, which are ozone treated to improve both electrochemical and mechanical performance compared with untreated CNT mat. The IL electrolyte can be dispensed locally into the electrode and separator layers to provide an electrochemically active supercapacitor region, which is fully encapsulated by the surrounding resin matrix during the cure cycle.

2 METHODS

The CNT mat used for functionalised interleave material and supercapacitor electrodes was supplied as 10-15 g m^{-2} Miralon Sheet (Huntsman, US). Oxygen functionalisation of the CNT mat was performed in an ultra-pure water bath enriched with ozone gas using a TG-20 ozone generator (Ozone solutions, US). CNT mat was functionalised for 1 h, 2 h, 6 h, 16 h and 22 h to be used in mechanical and electrochemical testing. Ozone-treated CNT mat was dried in a vacuum oven at 80°C for 1 hour.

A series of carbon fibre composites was produced with supercapacitor component materials laid up into the centre ply region, with increasing complexity towards the final design of the composite SSC. The composites use CYCOM IM7/977-3 unidirectional carbon fibre prepreg (Solvay, BE) as the host composite and 50 g m^{-2} CYCOM 1080/977-3 plain weave glass fibre prepreg (Solvay, BE) as the separator. The localised symmetrical supercapacitor SSC consists of two plies of 100 x100 mm CNT mat electrodes separated by one ply of 1080/977-3 glass fibre. The glass fibre had the pre-impregnated resin mostly dissolved out in a 25 mm diameter region in the centre of the fabric with methyl ethyl ketone solvent. 50 µL of 1-Ethyl-3-methylimidazolium bis(trifluoromethylsulfonyl)imide (EMIm TFSI) IL electrolyte was dropped into each of the electrodes and the centre of the glass fibre during the layup of the composite. Additional plies of carbon prepreg were laid up in equal amounts on either side of the SSC device to donate resin to the dry components of the SSC and stiffen the structure. Conventional vacuum bagging and autoclave curing was performed at 180 °C and 600 kPa for 8 hours.[12]

Another iteration of the composite SSC used an improved boron nitride nanotube (BNNT) separator [16], which was prepared to show improvements that were possible when the distance between the electrodes was reduced. The composite SSC was manufactured with autoclave cure times and temperatures described above. This composite SSC was electrochemically tested using a VMP3 potentiostat (BioLogic, FR) in a 25°C conventional oven. All of the initial electrochemical results were obtained from a single composite SSC with total electrode mass of 18.5 mg. Formulas for electrochemical calculations of galvanostatic charge/discharge (GCD) experiments for specific energy, E, and specific power, P, are:

$$E = \frac{i}{m}\int_0^t V \, \mathrm{d}t \qquad\qquad P = \frac{E}{t}$$

where *i* is the charge/discharge current *t* is time, *V* is the potential difference of the discharge curve not including the IR drop. [17]

3 RESULTS AND DISCUSSION

Composite panels with only a CNT mat interleave were tested to understand the impact of adding continuous sheets of the CNT mat across the entire structure and adding IL electrolyte to select locations to electrochemically activate the CNT mat as electrodes. It was important to understand whether the addition of the CNT mat would have a significant impact on the interlaminar shear strength, as

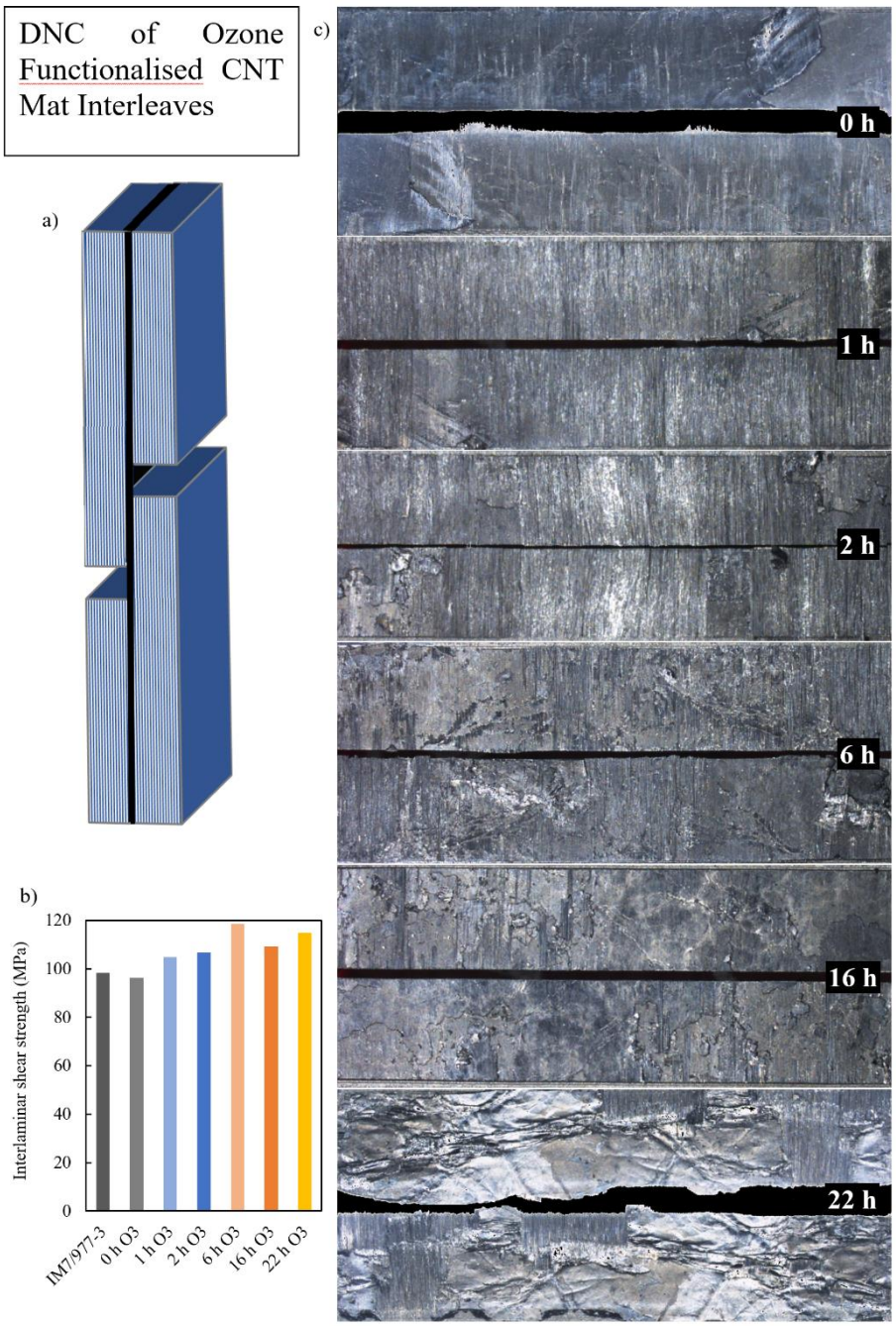

Figure 1: DNC testing of high-performance carbon fibre composite with functionalised CNT mat interleaves with a) diagram of test coupon, b) interlaminar shear strength including carbon fibre composite baseline and c) optical microscopy images of DNC coupons fracture surfaces.

delamination originating from the localised SSC would be the most-likely type of damage initiation. By implication, improving the CNT mat as a structural interleave should structurally reinforce the interply regions surrounding a localised SSC.

Interlaminar shear strength testing was performed using a high-performance carbon fibre composite with a CNT mat with increasing amounts of ozone functionalisation as an interleave. The use of the ASTM D695 standard test with D695 test fixture from Wyoming Test Fixtures along with high tolerance machining of the double-notch compression (DNC) coupons ensured a valid test was achieved with failure initiated in the mid ply of the panel, Fig. 1a. Initial interlaminar shear strength results are shown in Fig. 1b, including a baseline value of IM7/977-3 carbon fibre. Fig. 1 c) shows the upper and lower pairs of mating fracture surfaces after failure.

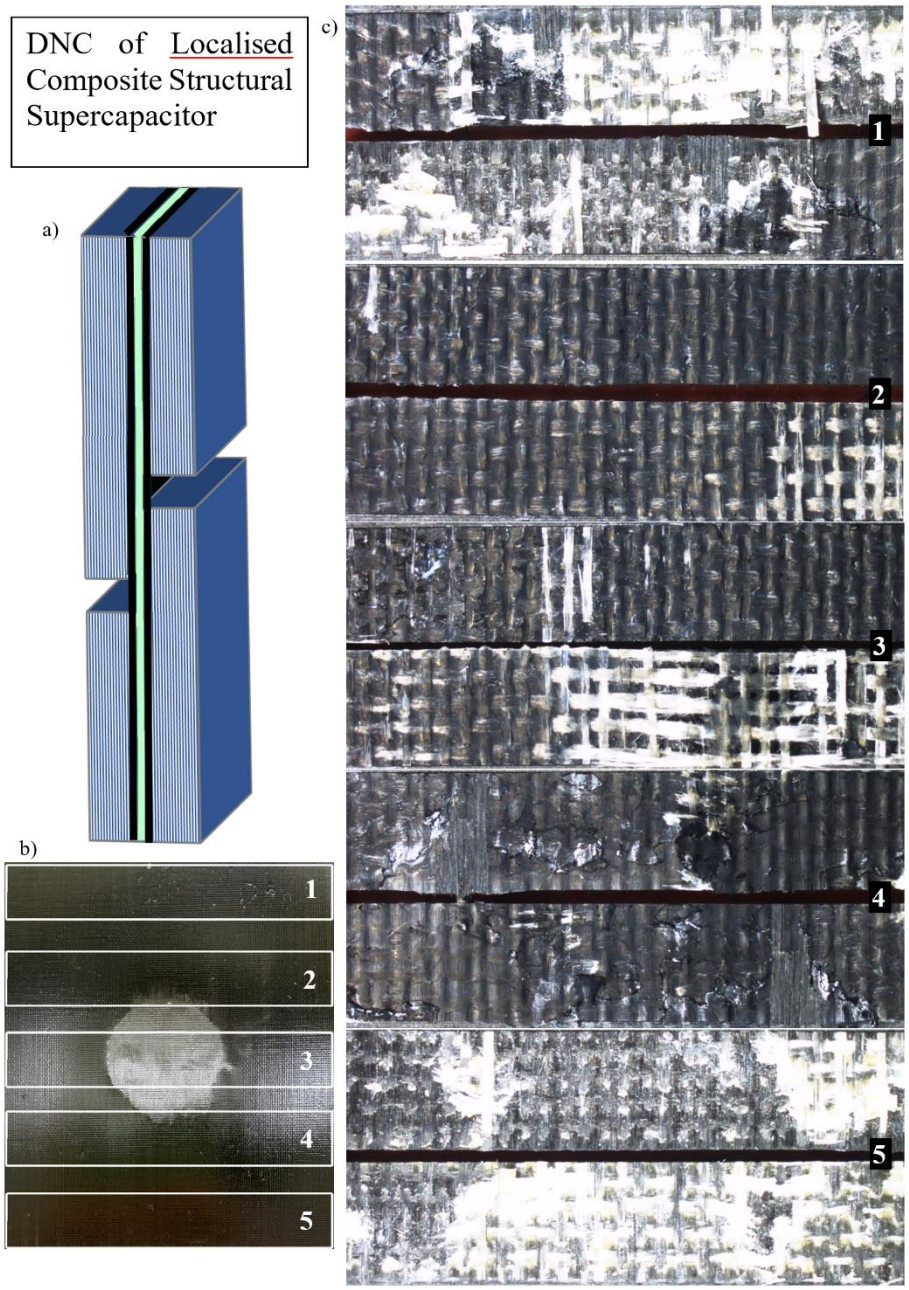

Figure 2: DNC testing of high-performance carbon fibre composite with localised SSC with a) diagram of test coupon, b) sampling diagram with SSC in the mid-plane and centre of the panel interleaves and c) optical microscopy images of composite SSC DNC coupons fracture surfaces.

The addition of untreated CNT mat showed a modest decrease in shear strength down to 96 MPa with failure clearly occurring in the bulk of the CNT mat. A layer of CNTs was seen to be well bonded to the carbon fibre potentially indicating limited diffusion of the resin into the CNT microstructure during cure. Then shear strength was seen to increase with ozone treatment time up to 6 hours, with a maximum shear strength of 118 MPa. The fracture surface of the 1 h and 2 h of ozonolysis samples showed fracture predominantly in the carbon fibre bulk with some failure at the CNT mat interface. Images in Fig. 1c of the 6 h sample show a mixture of failure in the carbon fibre, CNT mat and interfaces. From electron microscopy fractography, it has been determined that the increased number of oxygen functional groups increased the interfacial strength of the CNT mat and resin. However, at ozone treatment times longer than 6 hours, the damage of the CNT atomic structure was sufficient to cause CNT cleaving at lower failure loads than the 6 hour ozone treated samples. This was seen in 16 h and 22 h ozone treated samples with failure predominantly in the CNT mat bulk, still maintaining high shear strengths of 115 MPa.

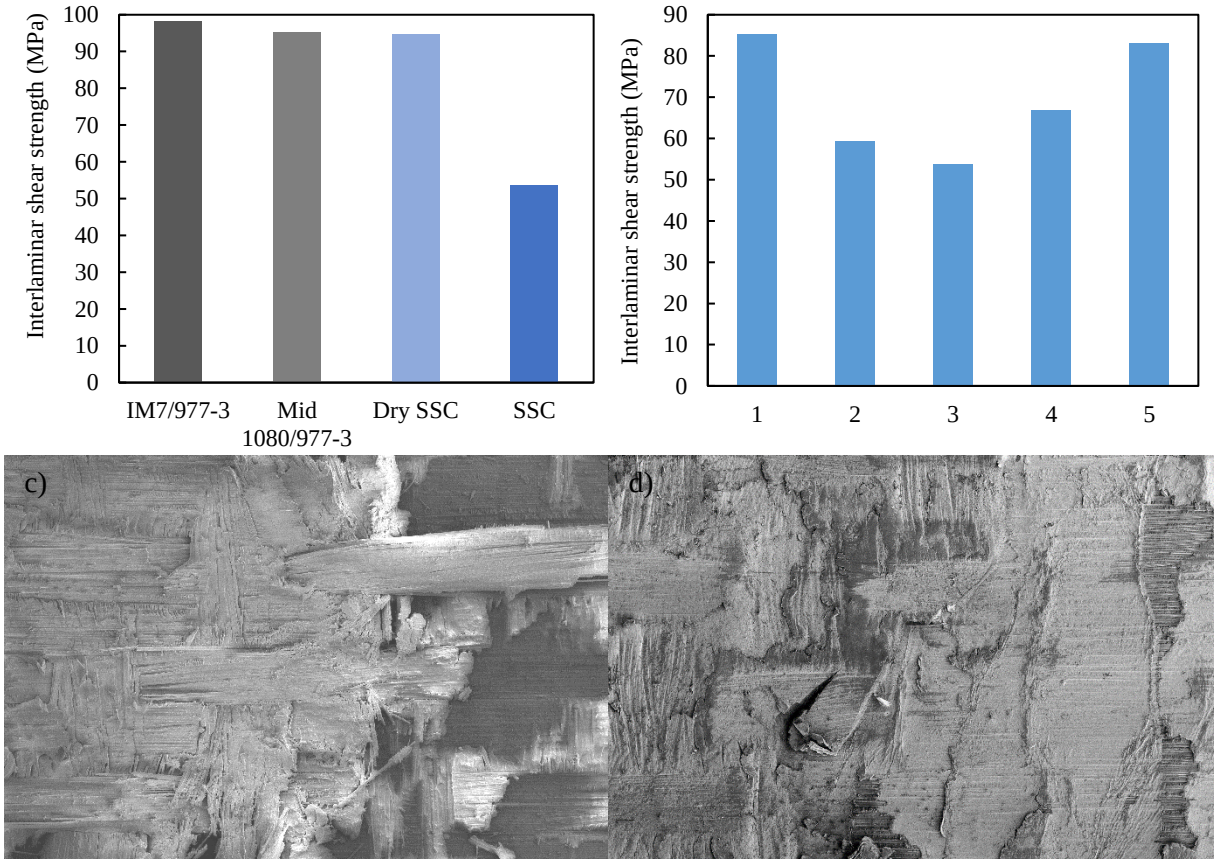

Figure 3: DNC testing of high-performance carbon fibre composite with supercapacitor components incorporated into the mid-ply region with a) interlaminar shear strength of carbon composite with glass, dry SSC and functional SSC with carbon baseline, b) interlaminar shear strength of coupons sampled across the composite with localised SSC as shown in Figure 3b, and electron microscopy images from c) Mid 1080/977-3 and d) dry SSC coupons.

Fig. 2 shows the different failure mechanisms at different locations in a composite with a localised SSC located in the centre. Fig. 2a shows the DNC coupons were accurately machined down to the SSC in the centre ply. Fig. 2b give a representation of how coupons 1-5 were sampled across the 100x100 mm composite panel. In Fig. 2c we can see images of coupons 1 to 5 of the DNC testing coupons described in Fig. 2b, showing upper and lower pairs of mating fracture surfaces after failure. Regions 1 and 5 represent areas away from the electrolyte and CNT mat electrodes of the supercapacitor. These regions remain mostly unaffected by the neighbouring SSC. Coupon 5 has failed predominantly in the interface between the glass and carbon plies. Region 1 contains CNT mat on one side of the coupon

leading to various failure zones including the glass interfaces and through the bulk of the CNT mat with shear strength above 83.0 MPa, Fig. 3b.

Region 2 and 4 are sampled in areas immediately adjacent to the SSC and is within the CNT mat electrode region so it may have some amount of IL electrolyte leak across into this region, reducing shear strength. These regions show failures in the CNT mat and carbon fibre interface as well as CNT mat bulk, however the right side of coupon 2 shows failure in the CNT mat-glass interface, which indicates this area was wet with IL electrolyte, reducing its strength to 59.2 MPa.

Region 3 is taken from the centre of the SSC where sufficient IL electrolyte is present to produce a high-energy supercapacitor. This region had the lowest interlaminar strength, which can be used as worst case strength values in modelling to design larger composite components. Imaging of this region showed the failure was contained predominantly within the glass fibre ply which only had limited remaining resin to form structural connections when curing. The interlaminar shear strength of coupon 3 was 53.8 MPa, which is relatively high considering the use of liquid electrolyte. This is due to

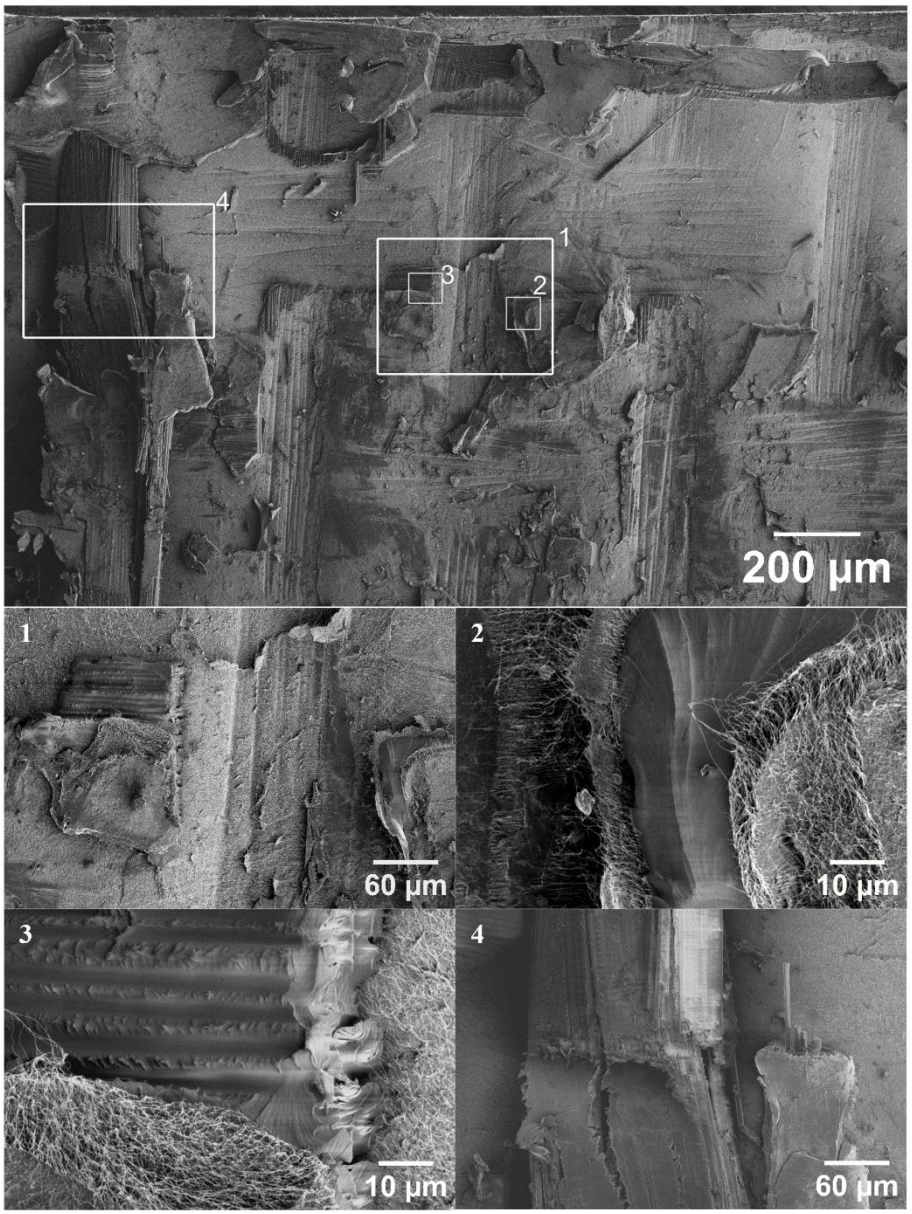

Figure 4: Electron micrograph of the composite SSC fracture surfaces of coupon 3 pictured in Figure 3c where the reference image locates the higher magnification features including 1) indentations left from woven glass fibre which has delaminated from the composite, 2) brittle fracture of resin region separating two CNT mat electrodes in hole region where neither warp or weft glass fibre tows cover, 3)

through thickness structural connection of horizontal fibres and 4) glass fibre tow infused predominantly with resin but also showing voids indicating the presence of IL.

formation of small structural connections formed through the glass fibre tows and adjacent to their intersection points in the composite, as detailed in Fig. 4.

Electron microscope images of the DNC coupons with glass fibre added as the middle ply to a laminate show the detrimental effects of adding a woven fabric into the high-performance unidirectional laminate, despite being manufactured with the same resin system, Fig. 3c. The shear performance of the composite has also been analysed with the addition of CNT mat electrodes and glass fibre separator with resin removed in the central region. This coupon is prepared without the addition of electrolyte to determine the worst case knockdown in shear strength without the inclusion of the electrolyte which is 94.7 MPa. As there is a significant strength knockdown in the SSC coupon with electrolyte added, it is important to determine the strengthening and failure mechanisms (as shown in the images Fig. 4).

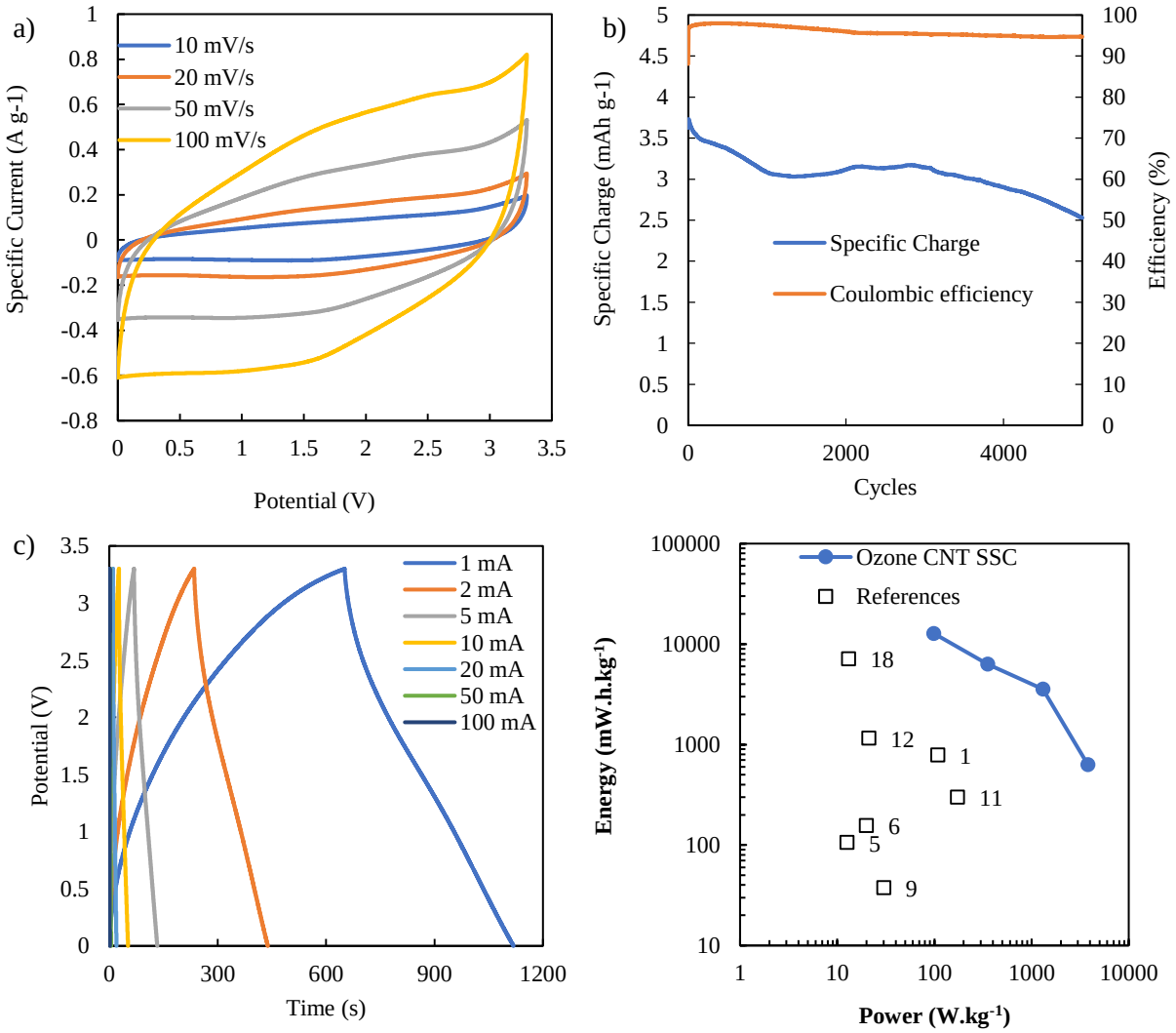

Figure 5: Electrochemical performance of localised structural supercapacitor with CNT-O6 electrodes, BNNT separator and EMIm TFSI electrolyte showing a) 3.3 V potential window with pseudocapacitive peaks 1 and 2.8 V, b) extended GCD cycling from 0 to 3.3 V at 1 A g^{-1} shows greater than 67 % capacitance retention with 95 % coulombic efficiency throughout cycling, c) shows good GCD performance from 1 mA to 100 mA currents corresponding to 0.0539 A g^{-1} to 5.39 A g^{-1}, and d) Ragone plot of specific energy and power compared to other composite SSCs with associated mechanical testing data. [1], [6], [6], [9], [11], [12], [18]

A typical fracture surface of SSC coupon 3 is shown in Fig. 4 top pane, showing a complicated mix of features which added to and subtracted from the strength of the composite. Image 1 from the reference image in Fig. 4 shows the critical region where two glass fibre tows overlap. In this region the vast majority of resin has been dissolved, however enough resin remains inside the glass fibre tows to bond the individual tows and intersections of tows together. Some of this resin will also flow into the CNT mat which is in contact with the tow. This will strengthen the glass ply in tension and compression but have less of an impact in shear. At the corners surrounding the intersections, excess resin is seen to provide a structural connection between both CNT mat electrodes as seen in Fig. 4 image 2 and 3. Image 2 shows both CNT mat electrodes connected by the 977-3 resin system, with resin seen to penetrate the electrodes even though they were impregnated with IL electrolyte when laid up. The clean fracture surface of this resin indicates it has not mixed significantly with the IL electrolyte and has, therefore, maintained its high strength. Image 4 also shows a similar feature where there are small regions of high concentrations of 977-3 resin providing structural connections through the active region of the composite SSC. Fig. 4 image 4 shows the state of the glass fibre tows which still contain enough resin within them to bond the tows together. Under test this tow appears to have experienced compressive and shear forces causing the tow to buckle laterally, leading to fibre breakage and a section of the tow to become disconnected. This shows the value of the developments made to localising SSCs within structural composites even with the use of liquid electrolytes. If the bulk of the resin had not been removed from the glass fibre prepreg separator material then this region would have insufficient ionic paths for the electrolyte to function, and if all of the resin was removed then no structural connections could be seen inside the device, reducing strength.

The development of the localised composite SSC materials and designs are ongoing with the goal to improving the electrochemical and mechanical reliability of the SSC cycling with vacuum-bag and autoclave curing process for high quality composites.[12] The following results are of one such newly developed SSC design including novel materials iterated from the previous localised SSC [12] and previously developed BNNT separator materials. [16] A 100 mm x100 mm composite device was manufactured with a 30 mm localised SSC that used electrodes of CNT treated for 6h in ozone as the cathode and anode, EMIm TFSI IL electrolyte and a BNNT separator. The electrode mass totalled 18.5 mg, with 90 µL of electrolyte. Initial electrochemical results of this new composite SSC design show very promising improvements over devices found in the literature. The cyclic voltammetry of the composite structural supercapacitor in Fig. 5a shows good charge storage with reversible pseudocapacitive peaks between 1 V and 2.8 V, which remain active at high cycling rates of 100 mV s^{-1}. There is no sign of unwanted chemical reactions with the polymer composite or any uncured monomers in the panel. The long term galvanostatic charge-discharge (GCD) cycling of the composite SSC, Fig 5b, cycling for 5000 cycles at 1 A g^{-1} shows good retention of the specific charge with coulombic efficiencies remaining above 94.6 %. In Fig. 5c the GCD cycling at different rates shows excellent performance from 1 mA to 100 mA currents corresponding to 0.0539 A g^{-1} to 5.39 A g^{-1}. The calculated equivalent series resistance (ESR) of 8.00 Ω from the 0.016 V potential drop (IR drop) in the 1 mA cycle and ESR of 8.45 Ω from the 1.69 V IR drop in the 100 mA cycle. The specific energy and power of this composite SSC are summarised in a Ragone plot in Fig. 5d, along with other high-performance composite SSC results in the literature, which had associated mechanical testing data. It can be seen that using ozone functionalised CNT electrodes in conjunction with BNNT separators has increased energy and ionic conductivity of the device. These electrochemical results are superior to other configurations, which will encourage the development of new materials and designs for composite SSCs.

4 CONCLUSIONS

Localised composite SSC with ozone functionalised CNT mat electrodes have been designed to maintain good electrochemical performance through the use of ionic liquid electrolytes, whilst maintaining moderate shear strengths in the active region with resin rich regions in the glass fibre ply. The shear strength of the composite is maintained at a high strength outside of the localised SSC through the use of 6 h ozone functionalised CNT mat electrodes, which readily infuse with the composite resin and form strong interfacial bonding with the cured matrix. The shear strength that has been retained in

the active SSC region is attributed to the remaining resin contained within the glass fibre separator ply forming small interlocking connection points with CNT mat electrodes. Electrochemical results of a composite SSC using 6 h ozone functionalised CNT mats as electrodes and BNNT separator is presented, which outperforms all other composite SSCs in supercapacitor performance with specific energy of 12.8 Wh kg^{-1} at 98.5 W kg^{-1} and specific power of 3790 W kg^{-1} at 0.632 Wh kg^{-1}.

REFERENCES

[1] A. Javaid and M. Irfan, Multifunctional structural supercapacitors based on graphene nanoplatelets/carbon aerogel composite coated carbon fiber electrodes, *Mater. Res. Express*, **6**, 2018, pp. 016310, (doi: 10.1088/2053-1591/aae862).

[2] N.S. Hudak, A.D. Schlichting, and K. Eisenbeiser, Structural Supercapacitors with Enhanced Performance Using Carbon Nanotubes and Polyaniline, *Journal of The Electrochemical Society*, 2017, pp. 11.

[3] Z. Sha *et al.*, Synergies of vertical graphene and manganese dioxide in enhancing the energy density of carbon fibre-based structural supercapacitors, *Composites Science and Technology*, **201**, 2021, pp. 108568, (doi: 10.1016/j.compscitech.2020.108568).

[4] E. Senokos, D.B. Anthony, N. Rubio, M.C. Ribadeneyra, E.S. Greenhalgh, and M.S.P. Shaffer, Robust Single-Walled Carbon Nanotube-Infiltrated Carbon Fiber Electrodes for Structural Supercapacitors: from Reductive Dissolution to High Performance Devices, *Advanced Functional Materials*, 2023, (doi: 10.1002/adfm.202212697).

[5] B.K. Deka, A. Hazarika, J. Kim, Y.-B. Park, and H.W. Park, Multifunctional CuO nanowire embodied structural supercapacitor based on woven carbon fiber/ionic liquid–polyester resin, *Composites Part A: Applied Science and Manufacturing*, **87**, 2016, pp. 256–262, (doi: 10.1016/j.compositesa.2016.05.007).

[6] B.K. Deka, A. Hazarika, Ob. Kwon, D. Kim, Y.-B. Park, and H.W. Park, Multifunctional enhancement of woven carbon fiber/ZnO nanotube-based structural supercapacitor and polyester resin-domain solid-polymer electrolytes, *Chemical Engineering Journal*, **325**, 2017, pp. 672–680, (doi: 10.1016/j.cej.2017.05.093).

[7] B.K. Deka *et al.*, Bimetallic copper cobalt selenide nanowire-anchored woven carbon fiber-based structural supercapacitors, *Chemical Engineering Journal*, **355**, 2019, pp. 551–559, (doi: 10.1016/j.cej.2018.08.172).

[8] B. Tynan, Y. Zhou, S.A. Brown, L. Dai, A.N. Rider, and C.H. Wang, Structural supercapacitor electrodes for energy storage by electroless deposition of MnO2 on carbon nanotube mats, *Composites Science and Technology*, **238**, 2023, pp. 110016, (doi: 10.1016/j.compscitech.2023.110016).

[9] E. Senokos *et al.*, Energy storage in structural composites by introducing CNT fiber/polymer electrolyte interleaves, *Scientific Reports*, **8**, 2018, (doi: 10.1038/s41598-018-21829-5).

[10] B.J. Mapleback, T.J. Simons, Y. Shekibi, K. Ghorbani, and A.N. Rider, Structural composite supercapacitor using carbon nanotube mat electrodes with interspersed metallic iron nanoparticles, *Electrochimica Acta*, **331**, 2020, pp. 135233, (doi: 10.1016/j.electacta.2019.135233).

[11] M. Rana, Y. Ou, C. Meng, F. Sket, C. González, and J.J. Vilatela, Damage-tolerant, laminated structural supercapacitor composites enabled by integration of carbon nanotube fibres, *Multifunct. Mater.*, **3**, 2020, pp. 015001, (doi: 10.1088/2399-7532/ab686d).

[12] B. Mapleback, V. Dao, L. Webb, and A. Rider, Composite Structural Supercapacitors: High-Performance Carbon Nanotube Supercapacitors through Ionic Liquid Localisation, *Nanomaterials*, **12**, 2022, pp. 2558, (doi: 10.3390/nano12152558).

[13] J. Schönherr, J. Buchheim, P. Scholz, and M. Stelter, Oxidation of carbon nanotubes with ozone and hydroxyl radicals, *Carbon*, **111**, 2017, pp. 631–640, (doi: 10.1016/j.carbon.2016.10.013).

[14] D. Iglesias *et al.*, Gas-Phase Functionalization of Macroscopic Carbon Nanotube Fiber Assemblies: Reaction Control, Electrochemical Properties, and Use for Flexible Supercapacitors, *ACS Appl. Mater. Interfaces*, **10**, 2018, pp. 5760–5770, (doi: 10.1021/acsami.7b15973).

[15] Q. An, A.N. Rider, and E.T. Thostenson, Electrophoretic deposition of carbon nanotubes onto carbon-fiber fabric for production of carbon/epoxy composites with improved mechanical properties, *Carbon*, **50**, 2012, pp. 4130–4143, (doi: 10.1016/j.carbon.2012.04.061).

[16] B.J. Mapleback *et al.*, Development of Stable Boron Nitride Nanotube and Hexagonal Boron Nitride Dispersions for Electrophoretic Deposition, *Langmuir*, **36**, 2020, pp. 3425–3438, (doi: 10.1021/acs.langmuir.0c00018).

[17] A. Noori, M.F. El-Kady, M.S. Rahmanifar, R.B. Kaner, and M.F. Mousavi, Towards establishing standard performance metrics for batteries, supercapacitors and beyond, *Chem. Soc. Rev.*, **48**, 2019, pp. 1272–1341, (doi: 10.1039/C8CS00581H).

[18] Y. Ding, G. Qi, Q. Cui, J. Yang, B. Zhang, and S. Du, High-Performance Multifunctional Structural Supercapacitors Based on In Situ and Ex Situ Activated-Carbon-Coated Carbon Fiber Electrodes, *Energy Fuels*, **36**, 2022, pp. 2171–2178, (doi: 10.1021/acs.energyfuels.1c03966).